Synthesis, Crystal Structure, DNA-binding Properties and Antioxidant Activities of a Lutetium(III) Complex with the Bis(*N*-salicylidene)-3-oxapentane-1,5-diamine Ligand

Guolong Pan, Yuchen Bai, Hua Wang, Jin Kong, Furong Shi, Yanhui Zhang, Xiaoli Wang, and Huilu Wu

School of Chemical and Biological Engineering, Lanzhou Jiaotong University, Lanzhou 730070, P. R. China

Reprint requests to Prof. Huilu Wu. E-mail: wuhuilu@163.com

Z. Naturforsch. **2013**, *68b*, 257 – 266 / DOI: 10.5560/ZNB.2013-2339
Received December 27, 2012

A Schiff base ligand bis(*N*-salicylidene)-3-oxapentane-1,5-diamine (H_2L) and its lutetium(III) complex, with composition $Lu_2(L)_2(NO_3)_2$, were synthesized and characterized by physico-chemical and spectroscopic methods. The crystal structure of the Lu(III) complex has been determined by single-crystal X-ray diffraction. It reveals a centrosymmetric binuclear neutral entity where Lu(III) metal centers are bridged by two phenoxo oxygen atoms. The DNA-binding properties of the Lu(III) complex were investigated by spectrophotometric methods and viscosity measurements, and the results suggest that the Lu(III) complex binds to DNA *via* a groove binding mode. Additionally, the antioxidant activity of the Lu(III) complex was determined by the superoxide and hydroxyl radical scavenging methods in *vitro*, which indicate that it is a scavenger for OH· and $O_2^{-\cdot}$ radicals.

Key words: Lutetium(III) Complex, Crystal Structure, DNA-Binding Properties, Antioxidant Activities, Bis(*N*-salicylidene)-3-oxapentane-1,5-diamine

Introduction

The interactions of metal complexes with DNA have been an active area of research at the interface of chemistry and biology [1 – 3]. Numerous biological experiments have demonstrated that DNA is the primary intracellular target of anticancer drugs. Interaction between small molecules and DNA can cause damage in cancer cells, blocking the division and resulting in cell death [4 – 6]. Particularly, some metal complexes are being used to bind and react at specific sequences of DNA in a search for novel chemotherapeutics, for probing DNA and for the development of highly sensitive diagnostic agents [7, 8]. Therefore, the research on the mechanism of the interaction of complexes with DNA is attracting more and more attention. The results will potentially be useful in the design of new compounds that can recognize specific sites or conformations of DNA [7 – 9].

Lanthanide metal complexes have been used as biological models to understand the structures of biomolecules and biological processes [10]. One of the most studied applications is the usage of the lanthanide complexes to address DNA/RNA by non-covalent binding and/or cleavage [11 – 14]. In addition, Schiff bases have been widely studied as they possess many interesting features, including photochromic and thermochromic properties, proton transfer tautomeric equilibria, biological and pharmacological activities, as well as suitability for analytical applications [15]. Now we give a full account of the synthesis, crystal structure, DNA-binding properties, and antioxidant activities of a Lu(III) complex with the Schiff base ligand bis(*N*-salicylidene)-3-oxapentane-1,5-diamine.

Experimental Section

Materials and physical measurements

All chemicals used were of analytical grade. Ethidium bromide (EB) and calf thymus DNA (CT-DNA) were purchased from Sigma-Aldrich and used without further purification. All the experiments involving interaction of the ligand and the complex with CT-DNA were carried out in doubly distilled water with a buffer containing 5 mM Tris

and 50 mM NaCl and adjusted to pH = 7.2 with hydrochloric acid. A solution of CT-DNA gave a ratio of UV absorbance at 260 and 280 nm of about 1.8 – 1.9, indicating that the CT-DNA was sufficiently free of protein [16]. The CT-DNA concentration per nucleotide was determined spectrophotometrically by employing an extinction coefficient of 6600 L mol^{-1} cm^{-1} at 260 nm [17].

C, H and N contents were determined using a Carlo Erba 1106 elemental analyzer. The IR spectra were recorded in the 4000 – 400 cm^{-1} region with a Nicolet FT-VERTEX 70 spectrophotometer using KBr pellets. Electronic spectra were taken on Lab-Tech UV Bluestar and Spectrumlab 722sp spectrophotometers. ^{1}H NMR spectra were obtained with a Mercury plus 400 MHz NMR spectrometer with TMS as internal standard and $CDCl_3$ as solvent. The fluorescence spectra were performed on a LS-45 spectrofluorophotometer at room temperature. Viscosity experiments were conducted on an Ubbelohde viscosimeter, immersed in a thermostated water bath maintained at 25.0 ± 0.1 °C.

Preparation of 3-oxapentane-1,5-diamine

3-Oxapentane-1,5-diamine was synthesized following the procedure in ref. [18]. – $C_4H_{12}N_2O$ (104.1): calcd. C 46.25, H 11.54, N 26.90; found C 45.98, H 11.50, N 26.76. – IR (KBr): ν = 1120 (C-O-C), 3340 (-NH_2) cm^{-1}.

Preparation of bis(N-salicylidene)-3-oxapentane-1,5-diamine (H_2L)

For the synthesis of H_2L, salicylic aldehyde (10 mmol, 1.22 g) in EtOH (5 mL) was added dropwise to 5 mL of an EtOH solution of 3-oxapentane-1,5-diamine (5 mmol, 0.52 g). After the completion of addition, the solution was stirred for an additional 4 h at 78 °C. After cooling to room temperature, the precipitate was filtered. The product was dried in *vacuo* and obtained as a yellow crystalline solid. Yield: 1.19 g (69 %). – $C_{18}H_{20}O_3N_2$ (312.4): calcd. C 69.21, H 6.45, N 8.97; found C 69.09, H 6.54, N 8.83. – UV/Vis (DMF): λ = 268, 316 nm. – IR (KBr): ν = 1286 (C-O-C); 1637 (C=N); 3458 (-OH) cm^{-1}. – ^{1}H NMR (400 MHz, $CDCl_3$): δ = 8.30 (s, 2H, N=C-H), 6.79 – 7.33 (m, 8H, H-benzene ring), 3.66 – 3.74 (m, 8H, O-(CH_2)$_2$-N=C).

Preparation of $Lu_2(L)_2(NO_3)_2$

To a stirred solution of H_2L (0.156 g, 0.5 mmol) in EtOH (10 mL) was added $Lu(NO_3)_3(H_2O)_6$ (0.191 g, 0.5 mmol) in EtOH (10 mL). A yellow sediment was generated rapidly. The precipitate was filtered off, washed with EtOH and absolute Et_2O, and dried *in vacuo*. The dried precipitate was dissolved in DMF to form a yellow solution. The yellow block-shaped crystals of $Lu_2(L)_2(NO_3)_2$ suitable for X-ray diffraction studies were obtained by vapor diffusion of diethyl ether into the solution for a few weeks at room temperature. Yield: 0.198 g (57 %). – $C_{36}H_{36}Lu_2N_6O_{12}$ (1094.6): calcd. C 39.46, H 3.29, N 7.67; found C 39.36, H 3.42, N 7.59. – UV/Vis: λ = 269, 317 nm. – IR (KBr): ν = 1243 (C–O–C); 1632 (C=N); 1385, 1058 (NO_3^-) cm^{-1}.

X-Ray crystallography

A suitable single crystal was mounted on a glass fiber, and the intensity data were collected on a Bruker Smart CCD diffractometer with graphite-monochromatized Mo K_α radiation (λ = 0.71073 Å) at 296(2) K. Data reduction and cell refinement were performed using the programs SMART and SAINT [19]. The absorption corrections were carried out empirically. The structure was solved by Direct Methods and refined by full-matrix least-squares against F^2 of data using the SHELXTL software package [20, 21]. The uncoordinated water molecule was found to be disordered. Its electron density was removed from the reflection intensities by using the routine SQUEEZE in PLATON. All H atoms were found in difference electron maps and were subsequently refined in a riding-model approximation with C–H distances ranging from 0.95 to 0.99 Å and U_{iso}(H) = 1.2 U_{eq}(C) or 1.5 U_{eq}(C). The crystal data and experimental parameters relevant to the structure determination are listed in Table 1. Selected bond lengths and bond angles are listed in Table 2.

Table 1. Crystal data and structure refinement for $Lu_2(L)_2(NO_3)_2$.

Complex	$Lu_2(L)_2(NO_3)_2$
Molecular formula	$C_{36}H_{36}Lu_2N_6O_{12}$
Molecular weight	1094.65
Color, habit	Yellow, block
Crystal size, mm^3	0.25 × 0.24 × 0.21
Crystal system	Monoclinic
Space group	$C2/c$
a, Å	29.177(11)
b, Å	11.652(5)
c, Å	15.236(6)
β, deg	119.115(3)
V, Å^3	4525(3)
Z	4
μ(Mo K_α), mm^{-1}	4.4
T, K	296(2)
$D_{calcd.}$, g cm^{-3}	1.61
F(000), e	2128
θ range data collection, deg	2.20 – 25.50
hkl range	±35, ±14, ±18
Reflections collected / unique / R_{int}	15 874 / 4214 / 0.0453
Data / restraints / parameters	4214 / 0 / 253
Final $R1$ / $wR2$ indices [$I > 2\sigma(I)$]	0.0273 / 0.0583
$R1$ / $wR2$ indices (all data)	0.0439 / 0.0635
Goodness-of-fit on F^2	0.957
Largest diff. peak / hole, e Å^{-3}	0.70 / −0.98

Table 2. Selected bond lengths (Å) and bond angles (deg) for $Lu_2(L)_2(NO_3)_2$.[a]

Bond lengths			
Lu(1)–O(3)	2.134(3)	Lu(1)–O(1)	2.427(3)
Lu(1)–O(2)#1	2.228(3)	Lu(1)–N(2)	2.431(4)
Lu(1)–O(2)	2.280(3)	Lu(1)–O(4)	2.441(3)
Lu(1)–O(5)	2.410(3)	Lu(1)–N(1)	2.455(4)
Bond angles			
O(3)–Lu(1)–O(2)#1	97.22(12)	O(2)–Lu(1)–O(1)	132.61(11)
O(3)–Lu(1)–O(2)	83.49(11)	O(5)–Lu(1)–O(1)	70.94(12)
O(2)#1–Lu(1)–O(2)	70.95(12)	O(3)–Lu(1)–N(2)	75.60(14)
O(3)–Lu(1)–O(5)	95.68(13)	O(2)#1–Lu(1)–N(2)	85.23(12)
O(2)#1–Lu(1)–O(5)	156.44(11)	O(2)–Lu(1)–N(2)	145.98(13)
O(2)–Lu(1)–O(5)	130.27(11)	O(5)–Lu(1)–N(2)	78.99(13)
O(3)–Lu(1)–O(1)	142.02(12)	O(1)–Lu(1)–N(2)	67.11(14)
O(2)#1–Lu(1)–O(1)	86.88(11)	O(3)–Lu(1)–O(4)	80.87(12)
O(2)#1–Lu(1)–O(4)	149.78(11)	O(2)–Lu(1)–O(4)	78.89(11)
O(5)–Lu(1)–O(4)	52.21(11)	O(1)–Lu(1)–O(4)	113.21(11)
N(2)–Lu(1)–O(4)	122.70(12)	O(3)–Lu(1)–N(1)	149.93(13)
O(2)#1–Lu(1)–N(1)	90.14(12)	O(2)–Lu(1)–N(1)	71.42(12)
O(5)–Lu(1)–N(1)	88.49(13)	O(1)–Lu(1)–N(1)	67.21(13)
N(2)–Lu(1)–N(1)	134.25(15)	O(4)–Lu(1)–N(1)	78.30(12)

[a] Symmetry transformations used to generate equivalent atoms: #1 $-x+1/2, -y+1/2, -z$.

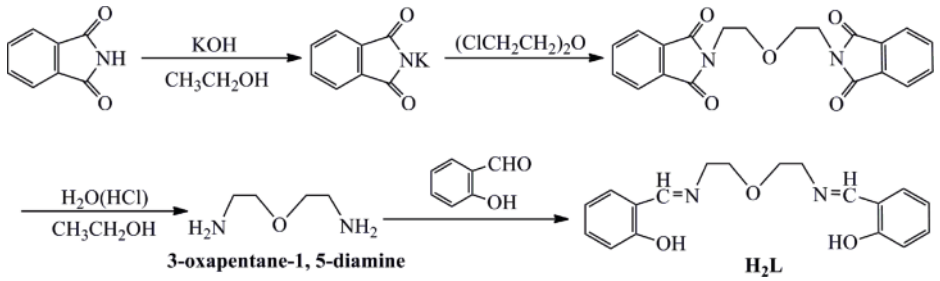

Scheme 1. Synthetic route for H_2L.

CCDC 916623 contains the supplementary crystallographic data for this paper. These data can be obtained free of charge from The Cambridge Crystallographic Data Centre *via* www.ccdc.cam.ac.uk/data_request/cif.

Results and Discussion

The synthetic route for the ligand precursor H_2L is shown in Scheme 1.

The Lu(III) complex $Lu_2(L)_2(NO_3)_2$ was prepared by reaction of H_2L with $Lu(NO_3)_3(H_2O)_6$ in ethanol. It is soluble in polar aprotic solvents such as DMF, DMSO and MeCN, slightly soluble in ethanol, methanol, ethyl acetate, and chloroform and insoluble in water, Et_2O and petroleum ether. The elemental analysis shows that its composition is $Lu_2L_2(NO_3)_2$ which was confirmed by the crystal structure analysis.

IR and electronic spectra

For the free ligand H_2L, a strong band is found at 1637 cm^{-1} together with a weak band at 1286 cm^{-1}. By analogy with previous assignments, the former can be attributed to ν(C=N), while the latter can be attributed to ν(C-O-C). These bands were shifted to lower frequencies by *ca.* 5 $\sim$ 43 cm^{-1} for the Lu(III) complex, which implies direct coordination of the nitrogen and oxygen atoms to the metal ion. Bands at 1385 and 1058 cm^{-1} indicate that nitrate is bidentate [22], in agreement with the result of X-ray diffraction.

The electronic spectra of the ligand H_2L and the Lu(III) complex were recorded in DMF solution at room temperature. The UV bands of H_2L (268, 316 nm) are marginally shifted in the complex. The two absorption bands are assigned to $\pi \rightarrow \pi^*$ (benzene) and $\pi \rightarrow \pi^*$ (C=N) transitions [23].

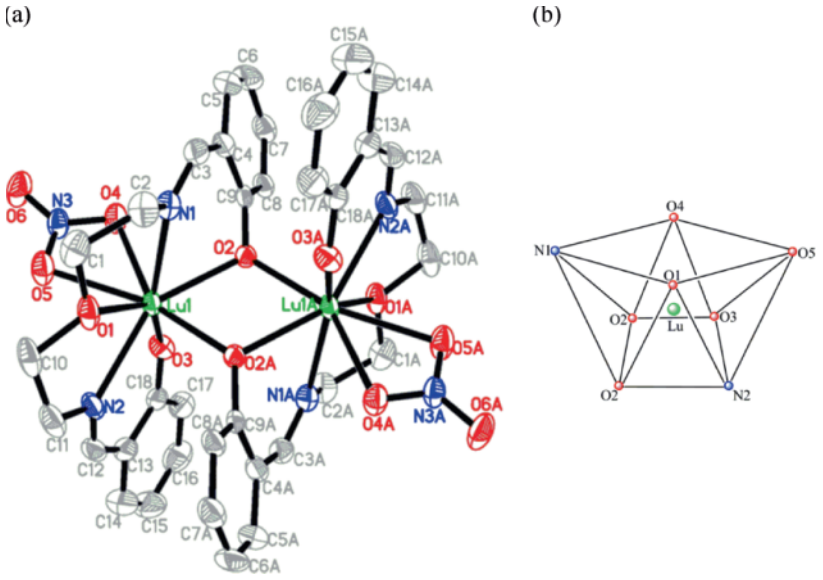

Fig. 1 (color online). (a) The molecular structure of the Lu(III) complex in the crystal with displacement ellipsoids at the 30 % probability level; H atoms are omitted for clarity; (b) a distorted square antiprism geometry is formed by the donor atoms around the Lu center as illustrated in the representation of the coordination polyhedron.

X-Ray structure of the complex

The prepared pentadentate ligand contains strong donors, namely phenoxo oxygen atoms as well as imine nitrogen atoms with an excellent coordination ability for transition/inner-transition metal ions through its N_2O_3 donor set. Single-crystal X-ray structure determination has revealed that the complex has a centrosymmetric neutral homobinuclear entity. An ORTEP illustration of the complex (Fig. 1a) shows that two adjacent [Lu(L)(NO_3)] moieties are bridged *via* two phenoxo groups. In the μ_2-diphenoxo bridged binuclear structure both Lu(III) centers are octa-coordinated. The local coordination environment is identical for both the centers by symmetry and is best described as a distorted square LuN_2O_6 antiprism (Fig. 1a). Due to the flexibility of the ligand, it loses its planarity (Fig. 1b). The bond lengths are in the range Lu(1)–N_{imine} 2.431(4) – 2.455(4), Lu(1)–O_{ether} 2.427(3) and Lu(1)–$O_{nitrate}$ 2.410(3) – 2.441(3) Å. The nature of coordination of the two Schiff base moieties of the same ligand is completely different. Of the two phenoxo oxygen atoms of each ligand, one is simply mono-coordinated while the other one bridges the adjacent Lu(III) centers as reflected by the Lu–$O_{phenoxo}$ bond lengths [Lu(1)–O(2) 2.280(3), Lu(1)–O(3) 2.134(3) Å]. The distance Lu(1)–Lu(1A) of 3.6711(14) Å is too long to consider any direct intramolecular Lu–Lu interaction. An interesting feature of this structure is the intermolecular hydrogen bond that exists among the Lu(III) complexes, which also leads to large solvent-accessible voids of 521 $Å^3$ which might trap guest molecules. Thus the solid may have the potential for practical applications such as gas absorption [24].

DNA-binding properties

Viscosity measurements

Hydrodynamic measurements that are sensitive to changes in DNA length are regarded as the least ambiguous and most critical tests of a binding model in solution in the absence of crystallographic data [25, 26]. In classical intercalation, the DNA helix lengthens as base pairs are separated to accommodate the bound complex, leading to increased DNA viscosity, whereas a partial, non-classical complex intercalation causes a bend (or kink) of the DNA helix and reduces its effective length and thereby its viscosity [27]. Viscosity experiments were conducted on an Ubbelohde viscosimeter, immersed in a water bath maintained at 25.0 ± 0.1 °C. Titrations were performed for the complex (3 – 30 μM), and the compound was introduced into CT-DNA solution (42.5 μM) present in the viscosimeter. Data were analyzed as $(\eta/\eta_0)^{1/3}$ *vs.* the ratio of the concentration of the compound to CT-DNA, where η is the viscosity of CT-DNA in the

presence of the compound and η_0 is the viscosity of CT-DNA alone. Viscosity values were calculated from the observed flow time of CT-DNA-containing solutions corrected for the flow time of buffer alone (t_0), $\eta = (t - t_0)$ [28].

Intercalating agents are expected to increase the viscosity of DNA because of a lengthening of the double helix due to the accommodation of the ligands in between the base pairs [29]. On the contrary, a partial and/or non-classical intercalation of the complex in the DNA grooves typically causes little (positive or negative) or no change in DNA solution viscosity [30]. The effects of H_2L and of the Lu(III) complex on the viscosity of CT-DNA is shown in Fig. 2. The experimental results have exhibited that the addition of ligand and complex causes no significant viscosity change, indicating that these compounds can bind to DNA in the groove mode.

Electronic absorption

The application of electronic absorption spectroscopy in DNA-binding studies is one of the most useful techniques [31]. Absorption titration experiments were performed with fixed concentrations of the complex, while gradually increasing the concentration of DNA. While measuring the absorption spectra, a proper amount of DNA was added to both the compound solution and the reference solution to eliminate the absorbance of DNA itself. In the UV region, the intense absorption bands observed for the ligand and for the complex are attributed to $\pi \rightarrow \pi^*$ transitions of the ligands. From the absorption titration data, the binding constant was determined using the following equation [32]:

$$[\mathrm{DNA}]/(\varepsilon_a - \varepsilon_f) = [\mathrm{DNA}]/(\varepsilon_b - \varepsilon_f) + 1/K_b(\varepsilon_b - \varepsilon_f)$$

where [DNA] is the concentration of DNA in base pairs, ε_a corresponds to the extinction coefficient observed ($A_{obsd}/[M]$), ε_f corresponds to the extinction coefficient of the free compound, ε_b is the extinction coefficient of the compound when fully bound to DNA, and K_b is the intrinsic binding constant. The ratio of slope to intercept in the plot of $[\mathrm{DNA}]/(\varepsilon_a - \varepsilon_f)$ *vs.* [DNA] gives the values of K_b. The absorption spectra of H_2L and of the Lu(III) complex in the absence and presence of CT-DNA are given in Fig. 3.

With increasing DNA concentrations, the absorption bands at 394 nm of H_2L show a hypochromism of 32 %; the absorption bands at 391 nm of the Lu(III) complex show a hypochromism of 63 %, suggesting that H_2L and the Lu(III) complex interact with CT-DNA [33]. The intrinsic binding constant K_b of H_2L and of the Lu(III) complex were 5.30×10^3 L mol^{-1} ($R = 0.99$ for 16 points) and 2.30×10^4 L mol^{-1} ($R = 0.99$ for 16 points), respectively, from the decay of the absorbances. The K_b values obtained here are lower than that reported for a classical intercalator (for ethidium bromide and [Ru(phen)DPPZ], binding constants are of the order of 10^6–10^7 L mol^{-1}) [34–37]. The

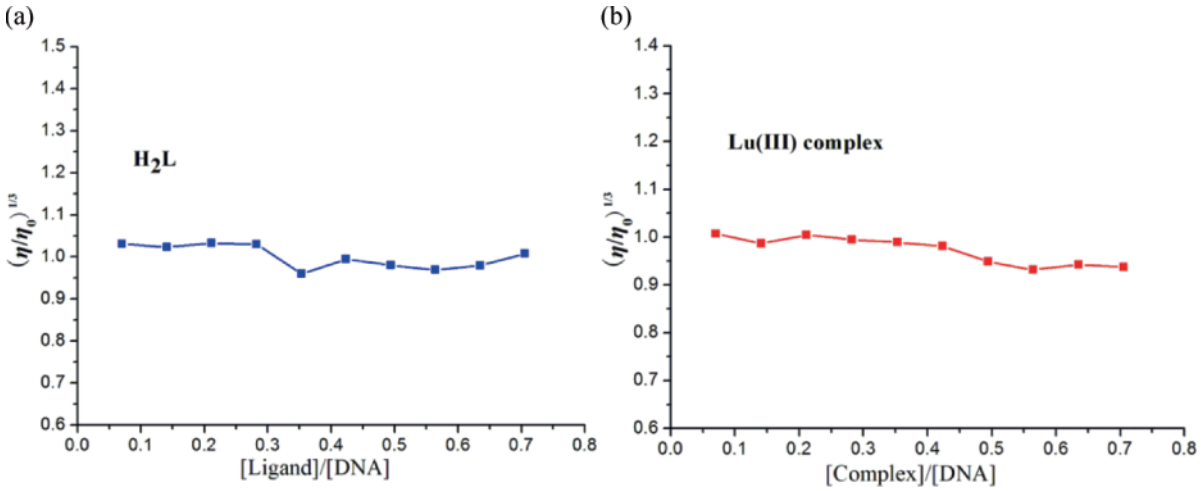

Fig. 2 (color online). Effect of increasing amounts of (a) H_2L and (b) Lu(III) complex on the relative viscosity of CT-DNA at 25.0 ± 0.1 °C.

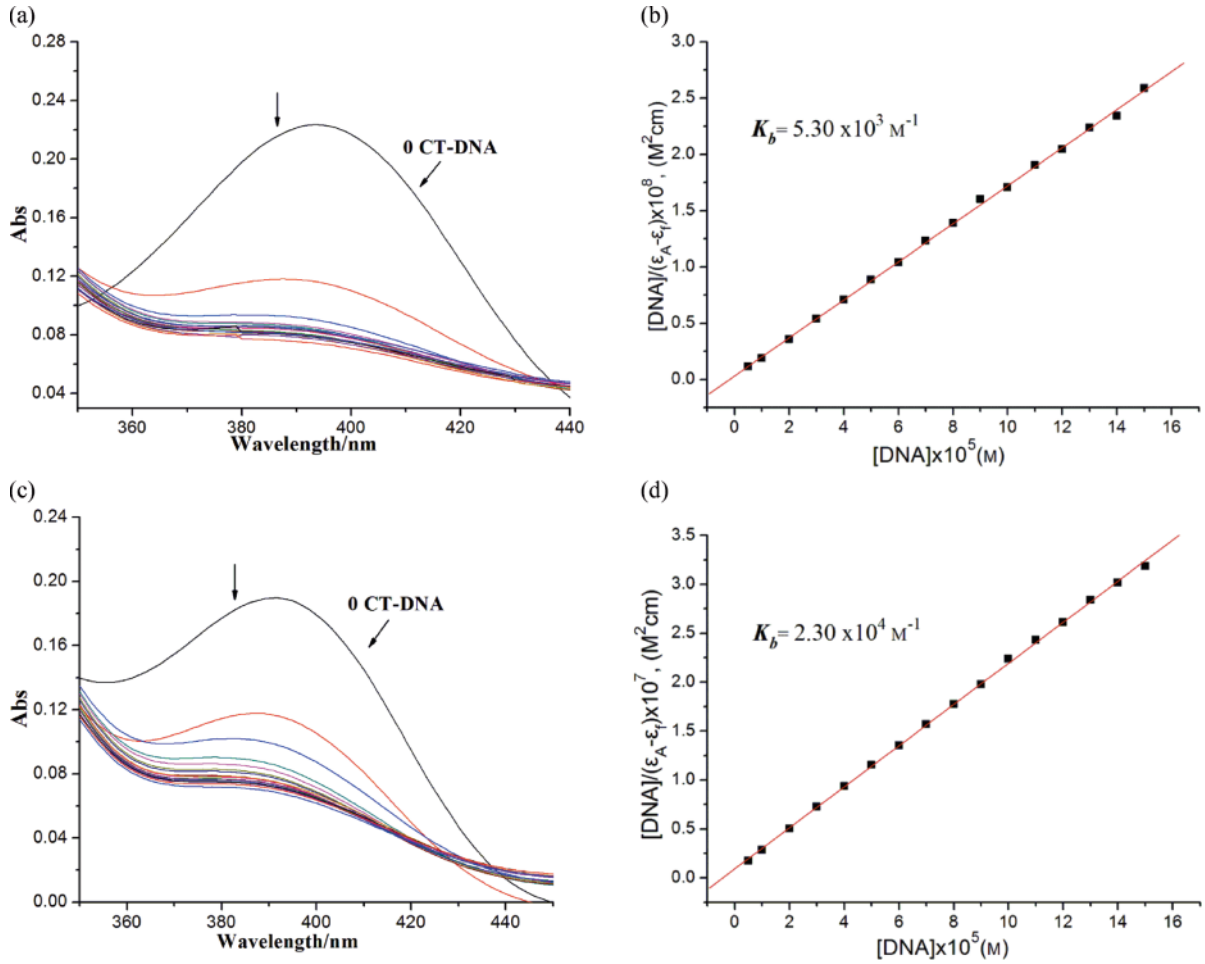

Fig. 3 (color online). Electronic spectra of (a) H_2L, (c) Lu(III) complex in Tris-HCl buffer upon addition of CT-DNA. [Compound] = 3.0×10^{-5} M, [DNA] = 2.5×10^{-5} M. Arrows show the emission intensity changes upon increasing the DNA concentration. Plots of [DNA]/(ε_a–ε_f) *vs.* [DNA] for the titration of (b) H_2L, (d) Lu(III) complex with CT-DNA.

hypochromism and the K_b values are not a strict evidence, but suggest an intimate association of the compounds with CT-DNA and indicate that the binding strength of the complex is higher than for H_2L.

Fluorescence spectra

No luminescence was observed for the complex at room temperature in aqueous solution, in the organic solvent examined and in the presence of calf thymus (CT-DNA). So the binding of the complex cannot be directly followed in the emission spectra. The enhanced fluorescence of EB in the presence of DNA can be quenched by the addition of a second molecule [38, 39]. To further clarify the interaction of the complex with DNA, a competitive binding experiment was carried out in a buffer by keeping [DNA]/[EB] = 1 and varying the concentrations of the complex. The fluorescence spectra of EB were measured using an excitation wavelength at 520 nm. The emission range was set between 550 and 750 nm. The spectra were analyzed according to the classical Stern-Volmer equation [40, 41]:

$$I_o/I = I + K_{sv}[Q]$$

where I_0 and$I$ are the fluorescence intensities at 599 nm in the absence and presence of the quencher, respectively, K_{sv} is the linear Stern-Volmer quenching con-

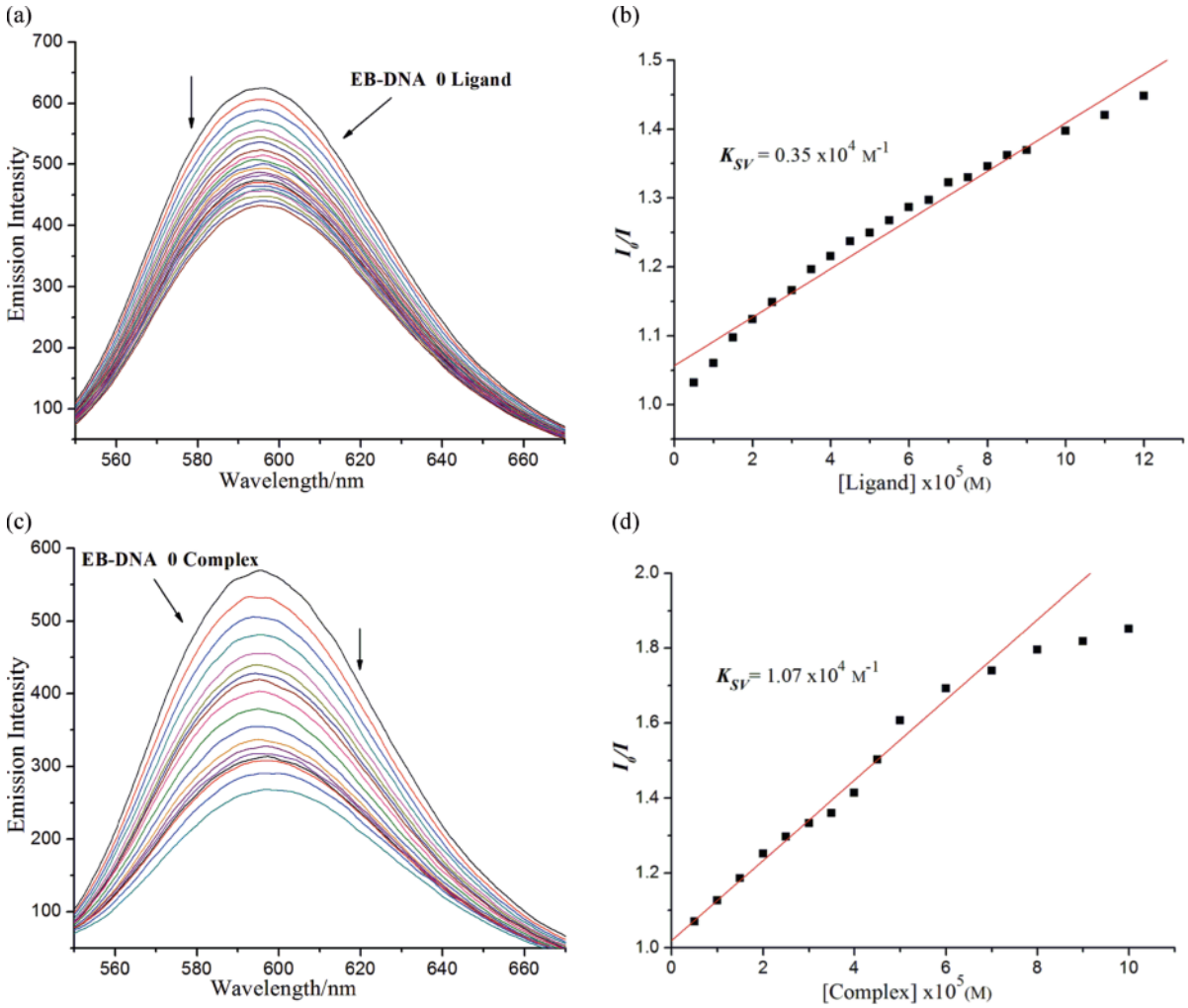

Fig. 4 (color online). Emission spectra of EB bound to CT-DNA in the presence of (a) H_2L and (c) Lu(III) complex; [Compound] $= 3.0 \times 10^{-5}$ M; $\lambda_{ex} = 520$ nm. The arrows show the intensity changes upon increasing the concentrations of the complexes. Fluorescence quenching curves of EB bound to CT-DNA by (b) H_2L and (d) Lu(III) complex. (Plots of I_0/I vs. [Complex]).

stant, and [Q] is the concentration of the quencher. The fluorescence quenching of EB bound to CT-DNA by H_2L and Lu(III) complex is shown in Fig. 4.

In general, measurements of the ability of a complex to affect the intensity of an EB fluorescence in the EB-DNA adduct allow the determination of the affinity of the complex for DNA, whatever the binding mode may be. If a complex can displace EB from DNA, the fluorescence of the solution will be reduced due to the fact that free EB molecules are readily quenched by the solvent water [42]. For the ligand H_2L and the Lu(III) complex, emission was observed neither for the components alone nor in the presence of CT-DNA in the buffer. The behavior of H_2L and of the Lu(III) complex is in good agreement with the Stern-Volmer equation, which provides further evidence that the two compounds bind to DNA. The K_{sv} values for H_2L and for the Lu(III) complex are 0.35×10^4 L mol^{-1} ($R = 0.98$ for 21 points in the line part) and 1.07×10^4 L mol^{-1} ($R = 0.99$ for 12 points), respectively, reflecting the higher quenching efficiency of the Lu(III) complex relative to that of H_2L.

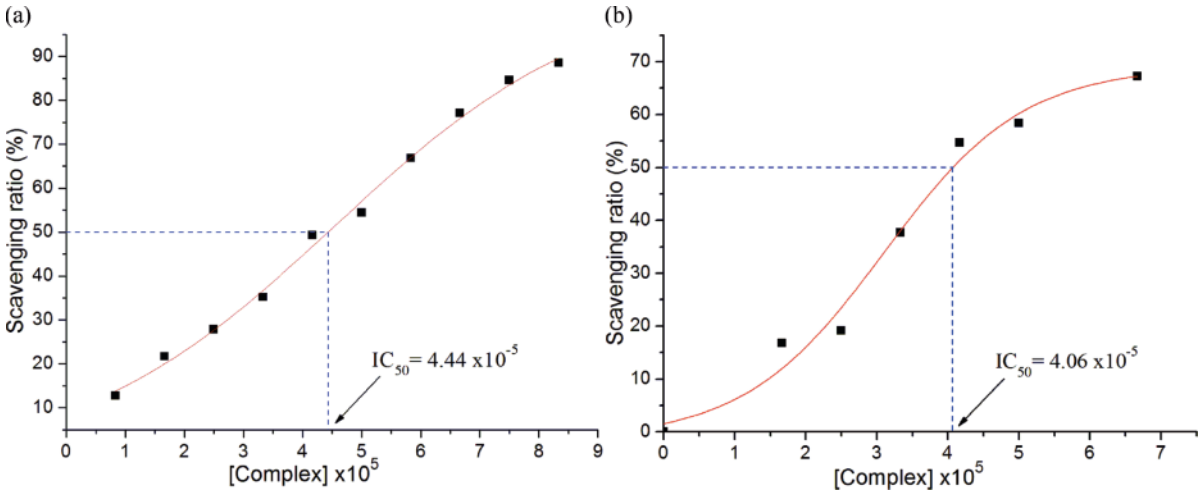

Fig. 5 (color online). Plots of antioxidation properties for the Lu(III) complex; (a) represents the hydroxyl radical scavenging effect (%) for the Lu(III) complex; (b) represents the superoxide radical scavenging effect (%) for the Lu(III) complex.

Antioxidant activities

Hydroxyl radical scavenging activity

Hydroxyl radicals were generated in aqueous media through the Fenton-type reaction [43, 44]. The reaction mixture (3 mL) contained 1 mL of 0.1 mmol aqueous safranin, 1 mL of 1.0 mmol aqueous EDTA-Fe(II), 1 mL of 3 % aqueous H_2O_2, and a series of quantitative microadditions of solutions of the test compound. A sample without the test compound was used as the control. The reaction mixtures were incubated at 37 °C for 30 min in a water bath. The absorbance was then measured at 520 nm. All the tests were run in triplicate, and the results are expressed as the mean and standard deviation (SD) [45]. The scavenging effect for OH· was calculated from the following expression:

$$\text{Scavenging ratio } (\%) = [(A_\text{i} - A_0) / (A_\text{c} - A_0)] \times 100\,\%$$

where A_i = absorbance in the presence of the test compound; A_0 = absorbance of the blank; A_c = absorbance in the absence of the test compound, EDTA-Fe(II) and H_2O_2.

We compared the ability of the present compound to scavenge hydroxyl radicals with those of the well-known natural antioxidants mannitol and vitamin C, using the same method as reported in a previous paper [46]. The 50 % inhibitory concentration (IC_{50}) value of mannitol and vitamin C are about 9.6×10^{-3} and 8.7×10^{-3} L mol^{-1}, respectively. According to the antioxidant experiments, the IC_{50} values of the Lu(III) complex is 4.44×10^{-5} L mol^{-1} (Fig. 5a), which implies that the complex exhibits better scavenging activity than mannitol and vitamin C.

Superoxide radical scavenging activity

A nonenzymatic system containing 1 mL 9.9×10^{-6} M VitB2, 1 mL 1.38×10^{-4} M NBT, 1 mL 0.03 M MET was used to produce the superoxide anion ($O_2^{-\cdot}$), and the scavenging rate of $O_2^{-\cdot}$ under the influence of 0.1 – 1.0 μM of the test compound was determined by monitoring the reduction in rate of transformation of NBT to monoformazan dye [47]. The solutions of MET, VitB2 and NBT were prepared with 0.02 M phosphate buffer (pH = 7.8) avoiding light. The reactions were monitored at 560 nm with a UV/Vis spectrophotometer, and the rate of absorption change was determined. The percentage inhibition of NBT reduction was calculated using the following equation [48]: percentage inhibition of NBT reduction = $(1 - k'/k) \times 100$, where k' and k present the slopes of the straight line of absorbance values as a function of time in the presence and absence of SOD mimic compound (SOD is superoxide dismutase), respectively. The IC_{50} values for the complexes were determined by plotting the graph of percentage inhibition of NBT reduction against the increase in

the concentration of the complex. The concentration of the complex which causes 50 % inhibition of NBT reduction is reported as IC_{50}.

The Lu(III) complex shows an IC_{50} value of 4.06×10^{-5} L mol^{-1} (Fig. 5b), which indicates that it has potent scavenging activity for the superoxide radical ($O_2^{-\cdot}$). The Lu(III) complex exhibits good superoxide radical scavenging activity and may be an inhibitor (or a drug) to scavenge superoxide radicals ($O_2^{-\cdot}$) *in vivo* which needs further investigation.

Conclusions

In summary, a novel Lutetium(III) complex based on the Schiff base ligand bis(*N*-salicylidene)-3-oxapentane-1,5-diamine has been synthesized and characterized. Its crystal structure has been determined by X-ray crystallography. The binding modes of the ligand and the complex with CT-DNA have been studied by electronic absorption titration, ethidium bromide-DNA displacement experiments and viscosity measurements. The results indicate that the Lu(III) complex shows higher affinity than the free ligand and interacts with CT-DNA through the groove mode. In addition, the antioxidant activities of the complex were investigated. The Lu(III) complex exhibited activities against $OH^{\cdot}$ and $O_2^{-\cdot}$ radicals in *in vitro* studies. Results obtained from our present work could be useful to understand the mechanism of interactions of small molecules with DNA and thus be helpful in the development of biological, pharmaceutical and physiological implications.

Acknowledgement

The authors acknowledge the financial support and grant from 'Qing Lan' Talent Engineering Funds by Lanzhou Jiaotong University. This work was also supported by the Fundamental Research Funds for the Universities (212086).

[1] C. P. Tan, J. Liu, L. M. Chen, S. Shi, L. N. Ji, *J. Inorg. Biochem.* **2008**, *102*, 1644 – 1653.
[2] K. E. Erkkila, D. T. Odom, J. K. Barton, *Chem. Rev.* **1999**, *99*, 2777 – 2795.
[3] I. C. Mendes, M. A. Soares, R. G. dos Santos, C. Pinheiro, H. Beraldo, *Eur. J. Med. Chem.* **2009**, *44*, 1870 – 1877.
[4] C. Hemmert, M. Pitie, M. Renz, H. Gornitzka, S. Soulet, B. Meunier, *J. Biol. Inorg. Chem.* **2001**, *6*, 14 – 22.
[5] V. S. Li, D. Choi, Z. Wang, L. S. Jimenez, M. S. Tang, H. Kohn, *J. Am. Chem. Soc.* **1996**, *118*, 2326 – 2331.
[6] G. Zuber, J. C. Quada, S. M. Hecht, *J. Am. Chem. Soc.* **1998**, *120*, 9368 – 9369.
[7] K. E. Erkkila, D. T. Odom, J. K. Barton, *Chem. Rev.* **1999**, *99*, 2777 – 2795.
[8] L. N. Ji, X. H. Zou, J. G. Lin, *Coord. Chem. Rev.* **2001**, 216/217, 513 – 536.
[9] B. M. Zeglis, V. C. Pierre, J. K. Barton, *Chem. Commun.* **2007**, *44*, 4565 – 4579.
[10] F. H. Lia, G. H. Zhao, H. X. Wu, H. Lin, X. X. Wu, S. R. Zhu, H. K. Lin, *J. Inorg. Biochem.* **2006**, *100*, 36 – 43.
[11] B. D. Wang, Z. Y. Yang, T. R. Li, *Bioorg. Med. Chem.* **2006**, *14*, 6012 – 6021.
[12] K. Wang, R. Li, Y. Cheng, B. Zhu, *Coord. Chem. Rev.* **1999**, *192*, 297 – 308.
[13] M. Marinić, I. Piantanida, G. Rusak, M. Žinić, *J. Inorg. Biochem.* **2006**, *100*, 288 – 298.
[14] Z. Y. Yang, B. D. Wang, Y. H. Li, *J. Organomet. Chem.* **2006**, *691*, 4156 – 4166.
[15] E. Hadjoudis, I. M. Mavridis, *Chem. Soc. Rev.* **2004**, *33*, 579 – 588.
[16] S. Satyanaryana, J. C. Dabrowiak, J. B. Chaires, *Biochem.* **1993**, *32*, 2573 – 2584.
[17] J. Marmur, *J. Mol. Biol.* **1961**, *3*, 208 – 218.
[18] S. M. Nalson, V. Knox, *Dalton Trans.* **1983**, 2525 – 2528.
[19] SMART, SAINT, Area Detector Control and Integration Software, Bruker Analytical X-ray Instruments Inc., Madison, Wisconsin (USA) **2000**; G. M. Sheldrick, SADABS, Program for Empirical Absorption Correction of Area Detector Data, University of Göttingen, Göttingen (Germany) **2002**.
[20] G. M. Sheldrick, SHELXTL, Siemens Analytical X-ray Instruments Inc., Madison, Wisconsin (USA) **1996**.
[21] G. M. Sheldrick, *Acta Crystallogr.* **2008**, *A64*, 112 – 122.
[22] K. Nakamoto. *Infrared and Raman Spectra of Inorganic and Coordination Compounds*, 4th ed., John Wiley & Sons, New York, **1986**, p. 284.
[23] L. Casella, M. Gullotti, A. Pintar, L. Messori, A. Rockenbauer, M. Györ, *Inorg. Chem.* **1987**, *26*, 1031 – 1038.
[24] M. J. Manos, M. S. Markoulides, C. D. Malliakas, G. S. Papaefstathiou, N. Chronakis, M. G. Kanatzidis, P. N. Trikalitis, A. J. Tasiopoulos, *Inorg. Chem.* **2011**, *50*, 11297 – 11299.

[25] J. R. Lakowicz, G. Webber, *Biochem.* **1973**, *12*, 4161 – 4170.
[26] M. Chauhan, K. Banerjee, F. Arjmand, *Inorg. Chem.* **2007**, *46*, 3072 – 3082.
[27] J. B. LePecq, C. Paoletti, *J. Mol. Biol.* **1967**, *27*, 87 – 106.
[28] M. Sethuraman, P. Mallayan, *Inorg. Chem.* **1998**, *37*, 693 – 700.
[29] Y. Li, Z. Y. Yang, M. F. Wang, *Eur. J. Med. Chem.* **2009**, *44*, 4585 – 4595.
[30] F. Chen, Z. Xu, P. Xi, X. Liu, Z. Zeng, *Anal. Sci.* **2009**, *25*, 359 – 363.
[31] H. L. Wu, Y. C. Gao, *Trans. Met. Chem.* **2004**, *29*, 175 – 179.
[32] Z. X. Su, Y. Q. Wan, H. L. Wu, *Synth. React. Inorg. Met. Org. Nano. Met. Chem.* **2005**, *35*, 553 – 558.
[33] K. Byunghoon, W. C. Ki, P. Myungho, S. L. Myoung, *Inorg. Chim. Acta* **1999**, *290*, 21 – 27.
[34] M. Cory, D. D. McKee, J. Kagan, D. W. Henry, J. A. Miller, *J. Am. Chem. Soc.* **1985**, *107*, 2528.
[35] M. J. Waring, *J. Mol. Biol.* **1965**, *13*, 269 – 282.
[36] V. G. Vaidyanathan, B. U. Nair, *J. Inorg. Biochem.* **2003**, *94*, 121 – 126.
[37] R. Vijayalakshmi, M. Kanthimathi, V. Subramanian, B. U. Nair, *Biochim. Biophys. Acta* **2000**, *1475*, 157 – 162.
[38] A. M. Pyle, J. P. Rehmann, R. Meshoyrer, C. V. Kumar, N. J. Turro, J. K. Barton, *J. Am. Chem. Soc.* **1989**, *111*, 3051 – 3058.
[39] S. Yellappa, J. Seetharamappa, L. M. Rogers, R. Chitta, R. P. Singhal, F. D'Souza, *Bioconjugate Chem.* **2006**, *17*, 1418 – 1425.
[40] A. Wolfe, G. H. Shimer, Jr., T. Meehan, *Biochem.* **1987**, *26*, 6392 – 6396.
[41] M. Shakir, M. Azam, M.-F. Ullah, S.-M. Hadi, *J. Photochem. Photobiol. B.* **2011**, *104*, 449 – 456.
[42] B. C. Baguley, M. Le Bret, *Biochem.* **1984**, *23*, 937 – 943.
[43] S. Satyanaryana, J. C. Dabrowiak, J. B. Chaires, *Biochem.* **1993**, *32*, 2573 – 2584.
[44] C. P. Tan, J. Liu, L. M. Chen, S. Shi, L. N. Ji, *J. Inorg. Biochem.* **2008**, *102*, 1644 – 1653.
[45] S. Satyanarayana, J. C. Dabrowiak, J. B. Chaires, *Biochem.* **1992**, *31*, 9319 – 9324.
[46] T. R. Li, Z. Y. Yang, B. D. Wang, D. D. Qin, *Eur. J. Med. Chem.* **2008**, *43*, 1688 – 1695.
[47] C. Beauchamp, I. Fridovich, *Anal. Biochem.* **1971**, *44*, 276 – 287.
[48] Q. H. Luo, Q. Lu, A. B. Dai, L. G. Huang, *J. Inorg. Biochem.* **1993**, *51*, 655 – 662.